Vietnam Journal of Catalysis and Adsorption
Tạp chí xúc tác và hấp phụ Việt Nam

https://chemeng.hust.edu.vn/jca/

Effect of metal–ligand ratio on the rhodamine B photodegradation activity of metal-organic framework materials based on bismuth and trimesic acid

Nguyen Duy Trinh[1,2*], Nguyen Huu Vinh[2], Pham Hoang Ai Le[3], Pham Quynh Trang[4], Tran Huu Huy[4], Tran Huu Quang[4], Nguyen Van Tuyen[4]

[1] *Graduate University of Scinece and Technology, Vietnam Academy of Science and Technology, 18 Hoang Quoc Viet street, Cau Giay, Ha Noi,Vietnam*
[2] *Institute of Applied Technology and Sustainable Development, Nguyen Tat Thanh University, Ho Chi Minh City, Vietnam*
[3] *Faculty of Chemical Engineering, Industrial University of Ho Chi Minh City, No. 12 Nguyen Van Bao, Ward 4, Go Vap District, Ho Chi Minh City,Vietnam*
[4] *Institute of Chemistry, Vietnam Academy of Science and Technology, 18 Hoang Quoc Viet street, Cau Giay, Ha Noi,Vietnam*
**Email: ndtrinh@ntt.edu.vn*

ARTICLE INFO

Received: 11/01/2022
Accepted: 18/4/2022
Published: 20/4/2022

Keywords:

Metal-organic framework, Metal–ligand ratio, Rhodamine b photodegradation

ABSTRACT

In this study, the photocatalytic degradation of rhodamine b (RhB) is investigated over metal-organic framework materials based on bismuth and trimesic acid (Bi-BTC) with different metal-to-ligand molar ratios. All obtained products are characterized by using powder X-ray diffraction, scanning electron microscopy, and UV–vis diffuse reflectance spectroscopy. It is found that decreasing the metal-to-ligand ratio below 1:1 produces high crystallinity and long rod-like crystals of Bi-BTC. For the metal-to-ligand molar ratios 5:1 and 1:1, we obtain low crystallinity of Bi-BTC. Additionally, a lower metal-to-ligand ratio in the Bi-BTC photocatalyst leads to the higher efficiency compared to other Bi-BTC photocatalysts. The metal-to-ligand ratio of 1:20 (Bi-BTC-0.05) favors the highest efficiency, in which 97.81% rhodamine B (RhB) is removed after 150 min of irradiation. The results should open a new approach to optimize the desired Bi-BTC structure for a target application.

Introduction

Metal-organic frameworks (MOFs) are currently attracting much attention from researchers because of their potential applications in the fields of adsorption, catalysis, and sensing. Therefore, the construction of new MOFs with diverse properties is being studied in practice and science. However, current studies focus on MOFs containing transition metals and lanthanides, [1,2] while only a few studies focus on main group metals.

Bismuth is a potential metal for building MOF structures thanks to its flexible coordination geometry and thus leads to the formation of diverse MOF structures. Recently, several bismuth-based MOFs with novel structures have been synthesized and shown to possess interesting photocatalytic and photocatalytic properties.[3–6] In particular, metal-organic framework

https://doi.org/10.51316/jca.2022.033

materials based on bismuth and trimesic acid (Bi-BTC) is currently being researched and applied widely in the field of photocatalysis and has shown high efficiency in the photocatalytic reaction to decompose organic dye.[7–9] However, due to the recombination of electrons and holes, the photocatalytic efficiency of the material is limited. Recently, researchers have enhanced the photocatalytic activity of Bi-BTC by combining with other materials. Specifically, Shuai-Ru Zhu et al. combined BiOBr with Bi-BTC to form a BiOBr/CAU-17 composite material with high photocatalytic activity to degrade organic dye.[10] Besides, the synthesis method to obtain materials with large surface area and/or high energy crystal surface also contributes to enhanced photocatalytic activity.[11] Our previous research showed that Bi-BTC has high photocatalytic activity, which is primarily determined by the solvent used in the synthesis process. Bi-BTC was synthesized by the thermal method using DMF/MeOH solvent mixture for the highest activity.[12] However, effect of metal–to-ligand molar ratio on the rhodamine b photodegradation activity of Bi-BTC has not been studied.

In this study, we synthesized Bi-BTC photocatalyst materials by hydrothermal method, using $Bi(NO_3)_3$ and trimesic acid as precursors with different Bi^{3+}/BTC^{3-} ratios in the solvent mixture of DMF/MeOH. The phase structure, crystal morphology, and light absorption properties of the materials were analyzed through XRD, SEM, and UV-Vis DRS methods. The photocatalytic activity of the as-synthesized Bi-BTC were studied through photocatalytic decomposition of rhodamine B (RhB) under white LED light irradiation.

Experimental

Materials

Bismuth (III) nitrate pentahydrate ($Bi(NO_3)_3 \cdot 5H_2O$, ≥ 98.0%), tri- mesic acid (H_3BTC, $C_9H_6O_6$, 95%), tert-butanol ($C_4H_{10}O$, ≥ 99.5%), rhodamine b ($C_{28}H_{31}ClN_2O_3$, ≥ 95%), and 1,4-benzoquinone ($C_6H_4O_2$, ≥ 99%) were purchased from Sigma-Aldrich. Sodium oxalate ($Na_2C_2O_4$, ≥ 99.8%), potassium dichromate ($K_2Cr_2O_7$, ≥ 99.8%), N,N- dimethylformamide (DMF, C_3H_7NO, 99%), and methanol (MeOH, CH_4O, ≥ 99.5%) were obtained from Xilong Scientific Co., Ltd.

Synthesis of Bi-BTC Photocatalysts

The solvothermal procedure employing $Bi(NO_3)_3 \cdot 5H_2O$ and H_3BTC as the precursors were adopted to synthesize the Bi-BTC samples.[13] Typically, x mmol of $Bi(NO_3)_3 \cdot 5H_2O$ and y mmol of H_3BTC (where x/y = 5:1, 1:1, 1:5, 1:10, 1:20, and 1:40; abbreviated as Bi-BTC-5, Bi-BTC-1, Bi-BTC-0.2, Bi-BTC-0.1, Bi-BTC-0.05, and Bi-BTC-0.025, respectively) were dispersed in 60 mL of MeOH/DMF solvent (MeOH/DMF volume ratio is 1:1). Then, the mixture was vigorously stirred for 30 min. Next, the transparent solution was transferred into a 100 mL solvothermal autoclave reactor. This autoclave was treated with 24 h of heating at 120 °C in an oven. The obtained white paste was rinsed with MeOH. Finally, the obtained powder was dried at 60 °C for 24 h.

Photocatalyst Characterization

X-ray diffraction (XRD) patterns of the synthesized samples were recorded in a D8 Advance Bruker powder diffractometer (Bruker, Billerica, MA, USA) with a Cu Kα excitation source. The surface morphologies of Bi-BTC samples were observed by scanning electron microscope (SEM, JEOL JSM 7401F, Peabody, MA, USA). UV–vis diffuse reflectance spectroscopy (UV-Vis DRS) was carried out on the Shimazu UV-2450 spectrometer (Shimazu, Kyoto, Japan).

Photocatalytic Reaction

The photocatalytic degradation of rhodamine B (RhB) over Bi-BTC samples were conducted in a 100 mL double-layer interbed glass beaker photocatalytic reactor under four daylight Cree® Xlamp® XM-L2 LEDs (max power of 10 W and max light output of 1052 lm) visible light irradiation. To perform this experiment, a mixture consisting of RhB aqueous solution (3×10^{-5} M, 50 mL) and the given catalyst (5 mg) was vigorously stirred for 60 min in the dark to ensure the adsorption–desorption equilibrium between the surface of Bi-BTC and the RhB molecules. During 150 min of photocatalytic processes, aliquots of the reaction solution was withdrawn at the same time intervals and the solid was immediately isolated by centrifugation to yield a transparent solution. The RhB concentration was determined by the change of the absorption intensity at its maximum absorbance wavelength of λ = 554 nm using a UV–visible spectrophotometer (Cary 60 UV–Vis, Agilent Technologies).

Results and discussion

https://doi.org/10.51316/jca.2022.033

Characterization of Bi-BTC samples

Figure 1 presents XRD patterns of the Bi-BTC samples. The variation of the metal-to-ligand ratio in a synthesis have affect on the crystal growth of Bi-BTC. The metal-to-ligand molar ratios 1:5, 1:10, 1:20, and 1:40 gave a Bi-BTC crystal phase with high crystallinity and was isomorphic to that of Bi-based MOF (CAU–17, CCDC 1426169).[7,13–16] For the metal-to-ligand molar ratios 1:1, we obtain low crystallinity of Bi-BTC. The deficient availability of H_3BTC ligands to form our target Bi-BTC was observed for the catalyst synthesis at the metal-to-ligand ratio 5:1.

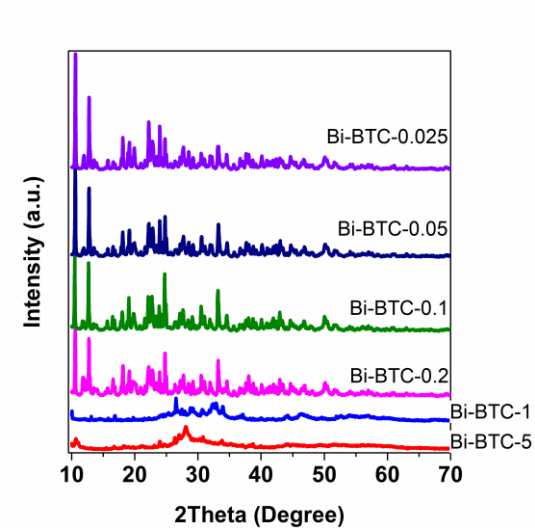

Figure 1: XRD pattern of Bi-BTC samples

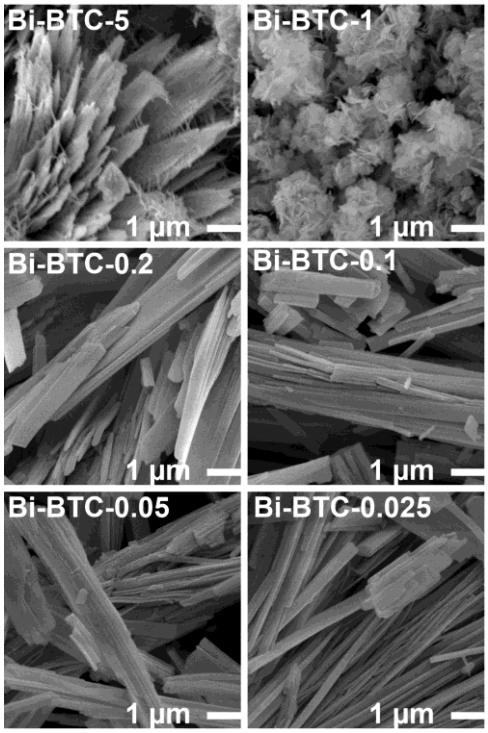

Figure 2: SEM images of Bi-BTC samples

The effect of metal–ligand ratio on the formation of Bi-BTC also considerably altered the morphology of the as-synthesized products, as exhibited in Fig 2. The morphology for the as-synthesized products at metal-to-ligand molar ratios 1:5, 1:10, 1:20, and 1:40 clearly shows the rod-like shape of the CAU-17 crystals formed.[16] The rod-like width obtained for Bi-BTC in those experiments vary in the range 200–300 nm. However, the morphology of the as-synthesized samples at the metal-to-ligand ratio 5:1 and 1:1 presents different morphology from those obtained at other molar ratios. Consistent with the results of the XRD patterns, the Bi-BTC-5 and Bi-BTC-1 (Figure 1) samples had low crystallinity.

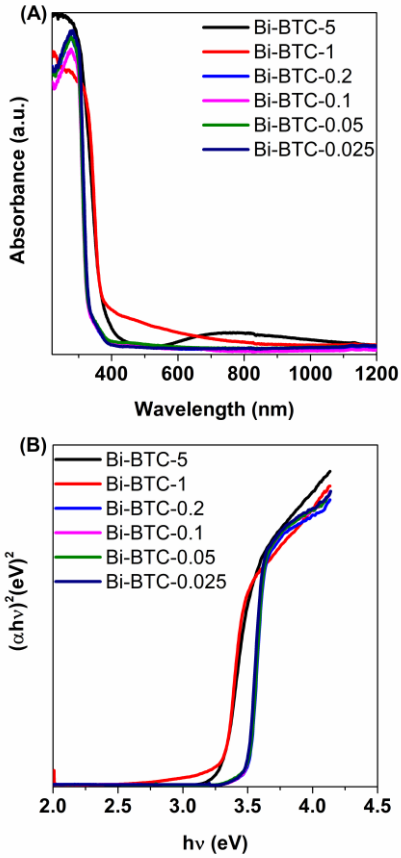

Figure 3: UV–Vis DRS spectra (A) and plots of $(\alpha h\nu)^2$ versus the photon energy ($h\nu$) (B) of Bi-BTC samples

UV-vis DRS spectra of all samples are displayed in Figure 3. The UV–visible absorption spectra show that in the both samples, there is absorption in the ultraviolet range with the absorption edges of 330–380 nm. The band gap energy (E_g) of the as-synthesized samples were derived from the tangent in the Tauc plots $\alpha h\upsilon = B(h\upsilon - E_g)^n$, where α is the absorption coefficient, $h\upsilon$ is the photon energy, B is the constant, E_g is the optical bandgap of the samples, and n is the constant,.[17] These materials belong to direct

bandgaps and n value in Tauc'equation is 1/2. The E_g values of the samples was determined to be 3.27 eV for Bi-BTC-5, 3.29 eV for Bi-BTC-1, and 3.49 eV for Bi-BTC-0.2, Bi-BTC-0.1, Bi-BTC-0.05 and Bi-BTC-0.025.

Photocatalytic activities of Bi-BTC samples under visible light

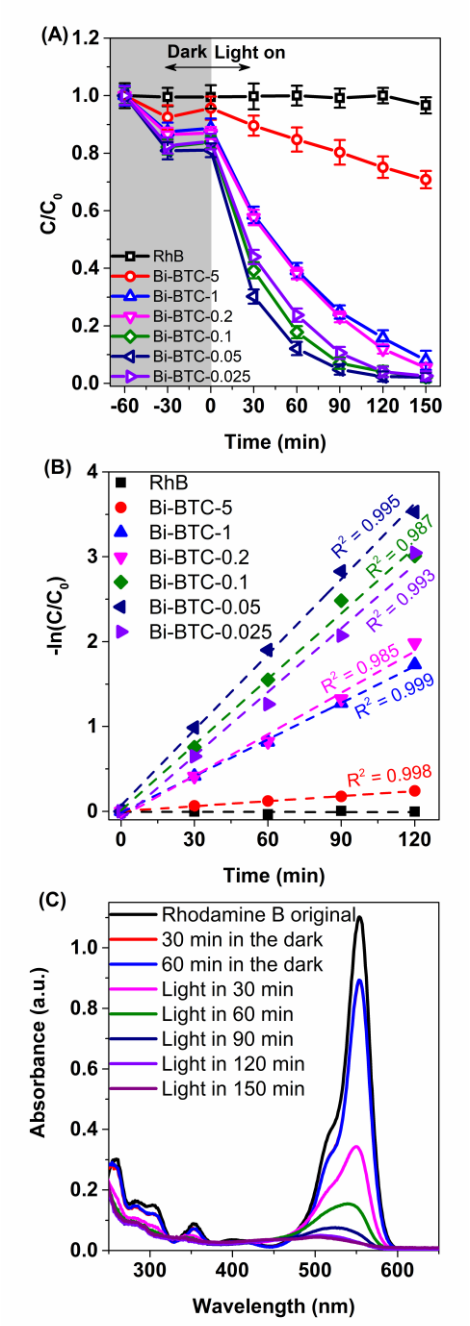

Figure 4: Photocatalytic degradation of RhB over Bi-BTC samples (A), plots of $\ln(C_0/C)$ versus irradiation time representing the fit using a pseudo-first-order reaction rate (B), and UV–Vis absorption spectra of RhB solution during illumination using Bi-BTC-0.05 (C)

To demonstrate the Effect of metal–ligand ratio on the photocatalytic activity of Bi-BTC, we conducted the photodegradation of RhB under white LED light irradiation. Fig 4A displays the removal efficiency of RhB by the as-synthesized samples. In comparison with the Bi-BTC-5 sample, the Bi-BTC synthesis at the metal-to-ligand ratio 1:1, 1:5, 1:10, 1:20, 1:40 exhibited significantly improved photocatalytic activity after 150 min of irradiation. The degradation rate of Bi-BTC-0.05 sample reached its highest value (about 97.8%) while the figure was 29.2% for the Bi-BTC-5 sample. In addition, the pseudo-first-order kinetic equation ($\ln(C/C_0) = kt$) was employed to fit the degradation of RhB (Fig 4B). The reaction rate constant (k) was determined to be 1.97×10^{-3} min^{-1} (Bi-BTC-5), 14.38×10^{-3} min^{-1} (Bi-BTC-1), 16.28×10^{-3} min^{-1} (Bi-BTC-0.2), 25.81×10^{-3} min^{-1} (Bi-BTC-0.1), 29.65×10^{-3} min^{-1} (Bi-BTC-0.05), and 25.05×10^{-3} min^{-1} (Bi-BTC-0.025), indicating that the Bi-BTC-0.05 sample exhibited superior photocatalytic performance. The Bi-BTC-0.05 sample has shown higher photocatalytic activity than earlier reports.[12,18]

Figure 4C shows UV-vis absorption spectra of RhB solution catalyzed by Bi-BTC-0.05 sample with respect to irradiation time. As shown in Fig 4C, the intensity of the absorption peak (554 nm) dramatically declined with increasing irradiation time and almost disappears when prolonging irradiation time to 150 min. These signs were attributed to the photodegradation of RhB molecules.

To elaborate on the mechanism for the active species responsible for RhB degradation over Bi-BTC-0.05, radical trapping experiments in the photodegradation were performed similar to the above photocatalytic activity test. Radical scavengers included 1,4-benzoquinone (BQ), potassium dichromate ($K_2Cr_2O_7$), sodium oxalate ($Na_2C_2O_4$), and tert-butanol (TBA) were agents that capture superoxide ($O_2^{\bullet-}$), electron (e^-), hole (h^+), and hydroxyl radicals ($HO^\bullet$), respectively. As displayed in Fig 5, the RhB photodegradation rate showed a marked decline follow the addition of $Na_2C_2O_4$ and BQ, implying that h^+ and $O_2^{\bullet-}$ species directly oxidized RhB molecules adsorbed on the surface of the Bi-BTC-0.05 catalyst.

To investigate the stability of the Bi-BTC-0.05 catalyst, the stability of the Bi-BTC-0.05 was tested three times by collecting and reusing the same photocatalyst and illustrated in Fig 6A. The photocatalytic activity of the Bi-BTC-0.05 sample is not significantly reduced after three runs, which may have been caused by the loss of the catalyst during the catalytic separation. Moreover,

there are no differences in the XRD of Bi-BTC-0.05 catalyst before/after three runs (Fig 6B), suggesting the excellent stability and reusability of the Bi-BTC-0.05 catalyst.

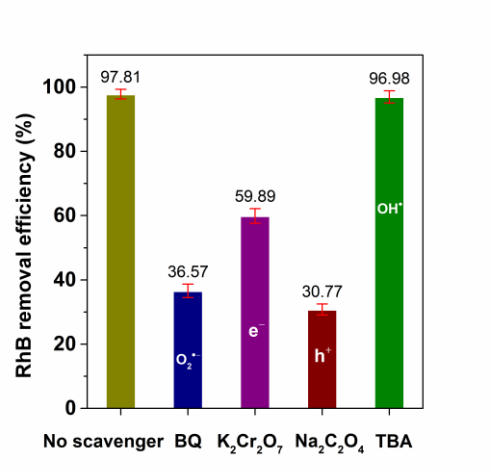

Figure 5: Trapping experiments of photocatalytic degradation of RhB over Bi- BTC-0.05sample

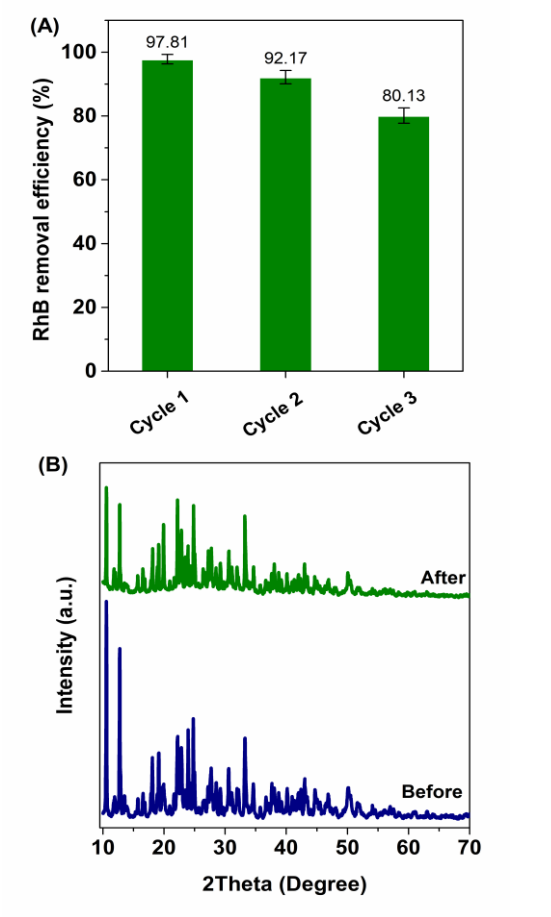

Figure 6: Photo-stability tests over Bi-BTC-0.05 sample for the cycling photodegradation of RhB (A) and XRD pattern of Bi-BTC-0.05 samples after and before photocatalytic reaction (B)

Conclusion

This study has shown that Bi-BTC has high photocatalytic activity and stability, which is primarily determined by the metal-to-ligand molar ratio used in the synthesis process. Bi-BTC was synthesized by the thermal method at the metal-to-ligand ratio of 1:20 (Bi-BTC-0.05) using DMF/MeOH solvent mixture favors the highest efficiency, 97.81% RhB is removed after 150 min of irradiation. Different metal-to-ligand molar ratio have influenced the crystal structure formation and different morphology of the as-synthesized products. Therefore, the photocatalytic efficiency of Bi-BTC was improved.

Acknowledgments

This research is funded by Graduate University of Science and Technology under Grant Number GUST.STS.ĐT2019-HH04.

References

1. K. Akhbari, A. Morsali, Mater Lett. 141 (2015) 315–318. https://doi.org/10.1016/j.matlet.2014.11.110.
2. P. George, N.R. Dhabarde, P. Chowdhury, Mater Lett. 186 (2017) 151–154. https://doi.org/10.1016/j.matlet.2016.09.099.
3. B. Yu, F. Wang, W. Dong, J. Hou, P. Lu, J. Gong, Mater Lett. 156 (2015) 50–53. https://doi.org/10.1016/j.matlet.2015.04.142.
4. J. Liu, J.-X. Hou, J.-P. Gao, J.-M. Liu, X. Jing, L.-J. Li, J.-L. Du, Mater Lett. 241 (2019) 184–186. https://doi.org/10.1016/j.matlet.2019.01.090.
5. K. Jiang, L. Zhang, Q. Hu, Y. Yang, W. Lin, Y. Cui, Y. Yang, G. Qian, Mater Lett. 225 (2018) 142–144. https://doi.org/10.1016/j.matlet.2018.05.006.
6. X. Gao, R. Cui, M. Zhang, Z. Liu, Mater Lett. 197 (2017) 217–220. https://doi.org/10.1016/j.matlet.2017.02.082.
7. R. Zhang, Y. Liu, Z. Wang, P. Wang, Z. Zheng, X. Qin, X. Zhang, Y. Dai, M.-H. Whangbo, B. Huang, , Appl Catal B Environ. 254 (2019) 463–470. https://doi.org/10.1016/j.apcatb.2019.05.024.
8. F. Ye, Z.-X. Wei, J.-F. Song, X.-H. Wu, P. Yue, Zeitschrift Für Anorg Und Allg Chemie. 643 (2017) 669–674. https://doi.org/10.1002/zaac.201700096.

9. M. Åhlén, E. Kapaca, D. Hedbom, T. Willhammar, M. Strømme, O. Cheung, Microporous Mesoporous Mater. 329 (2022) 111548. https://doi.org/10.1016/j.micromeso.2021.111548.

10. S.-R. Zhu, M.-K. Wu, W.-N. Zhao, P.-F. Liu, F.-Y. Yi, G.-C. Li, K. Tao, L. Han, Cryst Growth Des. 17 (2017) 2309–2313. https://doi.org/10.1021/acs.cgd.6b01811.

11. S.-M. Zhou, D.-K. Ma, P. Cai, W. Chen, S.-M. Huang, Mater Res Bull. 60 (2014) 64–71. https://doi.org/10.1016/j.materresbull.2014.08.023.

12. V.H. Nguyen, L. Van Tan, T. Lee, T.D. Nguyen, Sustain Chem Pharm. 20 (2021) 100385. https://doi.org/10.1016/j.scp.2021.100385.

13. A.K. Inge, M. Köppen, J. Su, M. Feyand, H. Xu, X. Zou, M. O'Keeffe, N. Stock, , J Am Chem Soc. 138 (2016) 1970–1976. https://doi.org/10.1021/jacs.5b12484.

14. M. Feyand, M. Köppen, G. Friedrichs, N. Stock, 19. Chem – A Eur J. 19 (2013) 12537–12546. https://doi.org/10.1002/chem.201301139.

15. M. Köppen, A. Dhakshinamoorthy, A.K. Inge, O. Cheung, J. Ångström, P. Mayer, N. Stock, Synthesis, Transformation, Eur J Inorg Chem. 2018 (2018) 3496–3503. https://doi.org/10.1002/ejic.201800321.

16. H. Ouyang, N. Chen, G. Chang, X. Zhao, Y. Sun, S. Chen, H. Zhang, D. Yang, Angew Chemie Int Ed. 57 (2018) 13197–13201. https://doi.org/10.1002/anie.201807891.

17. Z. Wu, X. Huang, H. Zheng, P. Wang, G. Hai, W. Dong, G. Wang, Appl Catal B Environ. 224 (2018) 479–487. https://doi.org/10.1016/j.apcatb.2017.10.034.

18. V.H. Nguyen, A.L.H. Pham, V.-H. Nguyen, T. Lee, T.D. Nguyen, Chem Eng Res Des 177 (2022) 321–330. https://doi.org/10.1016/j.cherd.2021.10.043.